Evidence for Charge-Controlled Conformational Changes in the Photocycle of Bacteriorhodopsin

H. J. Sass,* R. Gessenich,* M. H. J. Koch,# D. Oesterhelt,§ N. A. Dencher,¶ G. Büldt,* and G. Rapp#

*Forschungszentrum Jülich, IBI-2, Structural Biology, D-52425 Jülich; #European Molecular Biology Laboratory, EMBL c/o Deutsches Elektronen Synchrotron, D-22603 Hamburg; §Max-Planck-Institut für Biochemie, D-82152 Martinsried; and ¶Institute of Biochemistry, Department of Physical Biochemistry, Darmstadt University of Technology, D-64287 Darmstadt, Germany

ABSTRACT The existence of two different M-state structures in the photocycle of the bacteriorhodopsin mutant ASP38ARG was proved. At pH 6.7 (0 to −6°C) a spectroscopic M intermediate (M_1) that does not differ significantly in its tertiary structure from the light-adapted ground state accumulates under illumination. At pH > 9 another state (M_2), characterized by additional pronounced changes in the Fourier transform infrared difference spectrum in the region of the amide I and II bands, accumulates. The M_2 intermediate trapped at pH 9.6 displays the same changes in the x-ray diffraction intensities under continuous illumination as previously described for x-ray experiments with the mutant ASP96ASN. These observations indicate that in this mutant the altered charge distribution at neutral pH controls the tertiary structural changes that seem to be necessary for proton translocation.

INTRODUCTION

Upon illumination, the integral membrane protein bacteriorhodopsin (BR) generates a proton gradient across the membrane of *Halobacterium salinarum* (for reviews see Oesterhelt et al., 1992; Ebrey, 1993; Lanyi, 1995). Conformational changes in the protein moiety and/or the chromophore retinal are assumed to be key elements of the light-driven proton pumping cycle of BR (Schulten and Tavan, 1978; Fodor et al., 1988; Dencher et al., 1989; Hauss et al., 1994; Haupts et al., 1997), which transfers a proton from the cytoplasmic to the extracellular side.

In the membrane BR is naturally arranged in two-dimensional crystalline arrays, the so-called purple membrane. Therefore structural investigations using electron crystallography, neutron and x-ray diffraction were successful. These experiments and the recent x-ray crystallographic work on 3D crystals of BR resulted in a ground-state model of the molecule with atomic resolution (Grigorieff et al., 1996; Kimura et al., 1997; Pebay-Peyroula et al., 1997). Furthermore, tertiary structural changes were identified with the transition to the M intermediate (Dencher et al., 1989; Koch et al., 1991; Nakasako et al., 1991; Subramaniam et al., 1993). Recently it was demonstrated that these structural changes also persist in the following intermediate of the photochemical cycle, the N state (Kamikubo et al., 1996; Vonck, 1996), as originally suggested by time-resolved synchrotron x-ray diffraction (Koch et al., 1991). Furthermore, it could be shown that the onset of the tertiary structural changes is correlated with the transition between two M states (Sass et al., 1997), called M_1 and M_2. The latter finding contrasts with predictions based on Fourier transform infrared (FTIR) investigations (Braiman et al., 1991; Souvignier and Gerwert, 1992; Hessling et al., 1997), which indicated that the largest structural changes, defined by difference bands in the amide I and II region, take place with the $M \rightarrow N$ transition for wild-type (wt) BR and with the $M \rightarrow M_N$ transition for the Asp96Asn BR (Sasaki et al., 1992). A state comparable in the amide regions to the M_N state, but with a deprotonated Asp96 (negative band at 1742 cm^{-1} in the FTIR difference spectrum), was detected for the wt BR incubated with guanidine hydrochloride (GuaHCl) and was therefore called M_G (Sass et al., 1997). In contrast to the additional changes in the amide regions of the M_G state compared to M_2, the same large structural changes for both states are detected by diffraction experiments.

To verify the x-ray results indicating that the large changes in the structure occur with the $M_1 \rightarrow M_2$ transition, we have investigated the appearance of the structural changes for the Asp38Arg-BR mutant, by both x-ray diffraction and FTIR spectroscopy. This mutant was chosen because it has a long-lived M state and pumps protons, even though there are no indications in the amide region of the FTIR difference spectrum for large structural alterations compared to the ground state (Riesle et al., 1996).

MATERIALS AND METHODS

X-ray diffraction experiments

Purple membranes (PMs) of the BR mutant Asp38Arg were isolated from *Halobacterium salinarum*, strain L33, transformed with the appropriate vector carrying the mutated bacterioopsin (BO) gene according to the standard protocol (Riesle et al., 1996). PM films for x-ray measurements were prepared by drying an aliquot of a 30 mg/ml PM suspension at 86% relative humidity (r.h.) on a mica window at room temperature to obtain an optical density around 6 at 568 nm. This ensures a reasonable signal-to-noise ratio for the diffraction experiments, while still allowing most of the BR molecules to accumulate in the M state during continuous illumination.

Received for publication 11 December 1997 and in final form 15 April 1998.

Address reprint requests to Dr. H. J. Sass, Forschungszentrum Jülich, IBI-2: Structural Biology, D-52425 Jülich, Germany. Tel.: +49-2461-61-2036; Fax: +49-2461-61-2020; E-mail: Jurgen@ibistr.dnet.kfa-juelich.de.

0006-3495/98/07/399/07 $2.00

The adjustment of the desired pH value and the incubation with GuaHCl were performed by overlaying 50 μl of 20 mM phosphate buffer (pH 6.7), 100 mM carbonate buffer (pH 9.6) or 1 M GuaHCl in 100 mM carbonate buffer (pH 9.6) on top of the PM film and incubating the sample in a humidity chamber at 100% r.h. for at least 12 h. After removal of the excess liquid from the films with filter paper, all samples were adjusted to 100% r.h. for an additional 12 h. Subsequently, PM films were enclosed in airtight sample cells.

X-ray diffraction patterns were recorded on beamline X13 of the EMBL/Hamburg (on the storage ring DORIS of the Deutsches Elektronen Synchrotron (DESY), using a linear position sensitive detector with delay line readout (Gabriel and Dauvergne, 1982) and the standard data acquisition system (Boulin et al., 1988). To avoid radiation damage, the sample was continuously translated vertically in the x-ray beam. A small solenoid-driven shutter protected the sample from unnecessary irradiation between data collection periods. The total exposure time did not exceed 600 s.

Steady-state illumination was performed with a halogen cold light source equipped with a light guide (Schott, Mainz, Germany). A wavelength bandpass from 500 nm to 800 nm was selected, using a combination of an OG515 long-pass and a KG1 short-pass filter (Schott). For the x-ray experiments, accumulation of the M state was checked by measuring the absorption spectra at thinner positions of the PM films with a diode array spectrometer (J&M, Aalen, Germany) installed at the beamline. For the optical measurements, the sample and illumination conditions were identical to the ones of the diffraction experiment. The temperature of the samples was adjusted by a stream of dry cool air.

X-ray diffraction data were background-subtracted and Lorentz-corrected by multiplying the experimental intensities with the corresponding values of the scattering vector s ($s = 2\sin\Theta/\lambda$, where 2Θ is the scattering angle and $\lambda = 1.5$ Å, the wavelength). Diffraction patterns of the PM films incubated at pH 6.7 or pH 9.6 or with 1 M GuaHCl (pH 9.6) were obtained from three different samples and at different temperatures, about -6°C, $+6$°C, and $+6$°C, respectively. The different patterns were scaled by using the sum of the integrated reflection intensities in the range from reflection (1, 1) to (5, 2). This procedure is, of course, not entirely accurate, as the samples might have developed different amounts of disorder.

Difference density maps with a resolution of 7 Å were calculated from the difference amplitudes of the illuminated and the light-adapted ground-state samples by using phases from electron microscopy (Henderson et al., 1986). The amplitudes of overlapping reflections were determined by splitting Lorentz-corrected intensities according to the electron microscopy data.

FTIR spectroscopy

For FTIR measurements, PM films of the BR mutant ASP38ARG were prepared by applying a 5-μl aliquot of a 10 mg/ml suspension to a CaF_2 window and allowing it to stand for a few minutes in air until most of the water was evaporated. Thereafter, the samples were adjusted to 100% r.h. by incubating them for at least 12 h over pure water in a humidity chamber. Subsequently, the samples were sealed with a greased Teflon spacer ring and a second CaF_2 window.

For incubation with GuaHCl, 20 μl of a 1 M solution (pH 9.6) was deposited on a PM film for at least 1 h at 100% r.h. Thereafter, the excess GuaHCl solution was removed with filter paper. The samples were stored at 100% r.h. before the cell was sealed as described above.

FTIR difference spectra were recorded with a Bruker IFS66V spectrometer after baseline stability was ensured. Difference spectra with a resolution of 2 or 4 cm^{-1} were obtained from the average of at least 100 scans in the dark and the average of the immediately following 100 scans under continuous illumination, using the same light source as for the x-ray measurements. All measurements were repeated at least three times. They were performed either at 20°C or at 10°C. For comparison, the spectra were scaled to the same difference absorbance value at 1201 cm^{-1}.

RESULTS AND DISCUSSION

X-ray diffraction and visible absorption spectroscopy

The ASP38ARG-BR photocycle intermediates, accumulated under various conditions, were characterized by visible and FTIR difference spectroscopy. For the exact control of the state of the sample, measurements in the visible wavelength region were performed under conditions identical to those in the diffraction experiment. The optical spectra of the ASP38ARG-BR sample at pH 6.7, 100% r.h., and of a sample incubated with GuaHCl, pH 9.6, are shown in Fig. 1. The absorption maxima around 410 nm clearly indicate the presence of a predominant fraction of M intermediate during illumination. Despite the fact that the absorption band of the ground state is distorted because of the response of the spectrometer, this conclusion can be drawn, because the ratio of the absorption bands of the illuminated sample (around 410 nm) to the light-adapted ground state

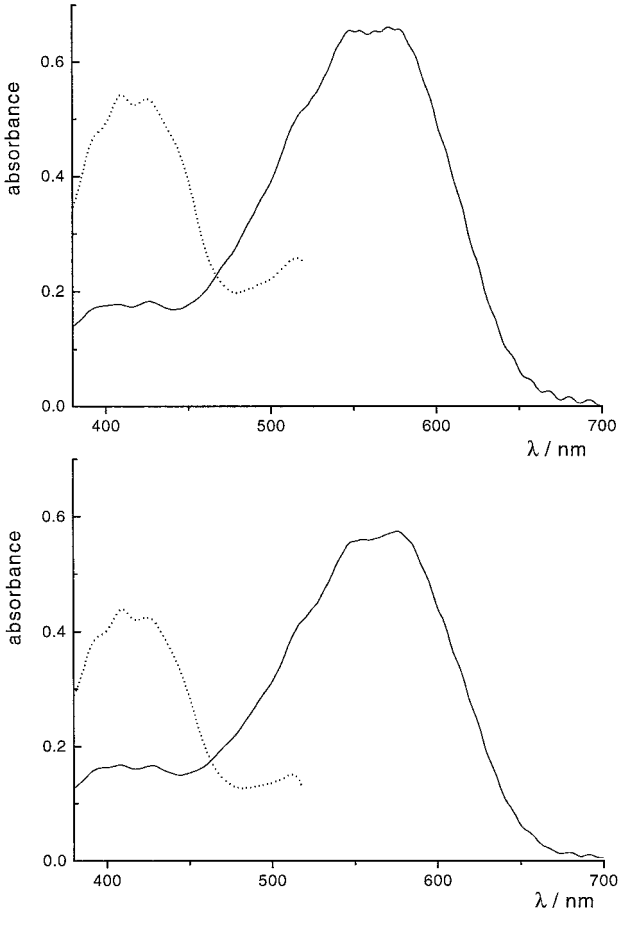

FIGURE 1 Optical spectra of the BR-ASP38ARG samples cooled to -6°C with (·····) and without (——) illumination as used for the diffraction experiment. The spectra of the ground state are slightly disturbed around the absorption maximum by the response of the spectrometer at such high OD. The spectra of the illuminated samples are only shown up to 520 nm, because the longer-wavelength part is disturbed by the excitation light. (*Top*) Sample at pH 6.7. (*Bottom*) Sample incubated with GuaHCl, pH 9.6.

(around 570 nm) is in the range of 0.7 for both samples. An absorption ratio of this amount is indicative for an accumulation of all molecules in the M intermediate (Nagle et al., 1982). These optical spectra were obtained by cooling both samples between −2° and −6°C. Only under this condition could most of the BR molecules of the pH 6.7 sample be trapped in the M intermediate under continuous illumination.

Diffraction patterns of a sample at pH 6.7, cooled just below 0°C, and of samples at pH 9.6 with and without GuaHCl, at +6°C, are shown in Fig. 2. Despite the large differences in the diffraction patterns, according to the optical measurements all three samples are in the M state when illuminated. Although background noise is high, it is evident that the sample at pH 6.7 does not diplay any significant changes in the intensities of the diffraction pattern under continuous illumination. On the other hand, clear differences are detectable between intensities of the ground state and the illuminated state of the samples at pH 9.6, with and without GuaHCl. In particular, the changes in the (3, 2) and (4, 1) reflections characteristic of the large tertiary structural changes associated with the transition to the M intermediate (Dencher et al., 1989; Koch et al., 1991) or, more precisely, to the M_2 intermediate (Sass et al., 1997) are clearly present in the diffraction patterns. Only the extent of the changes is different in the two samples at pH 9.6, because the number of molecules in the M intermediate is expected to be slightly smaller without than with GuaHCl at the measuring temperature of about +6°C. This is reasonable because optical measurements show that without the addition of GuaHCl, the number of molecules accumulated

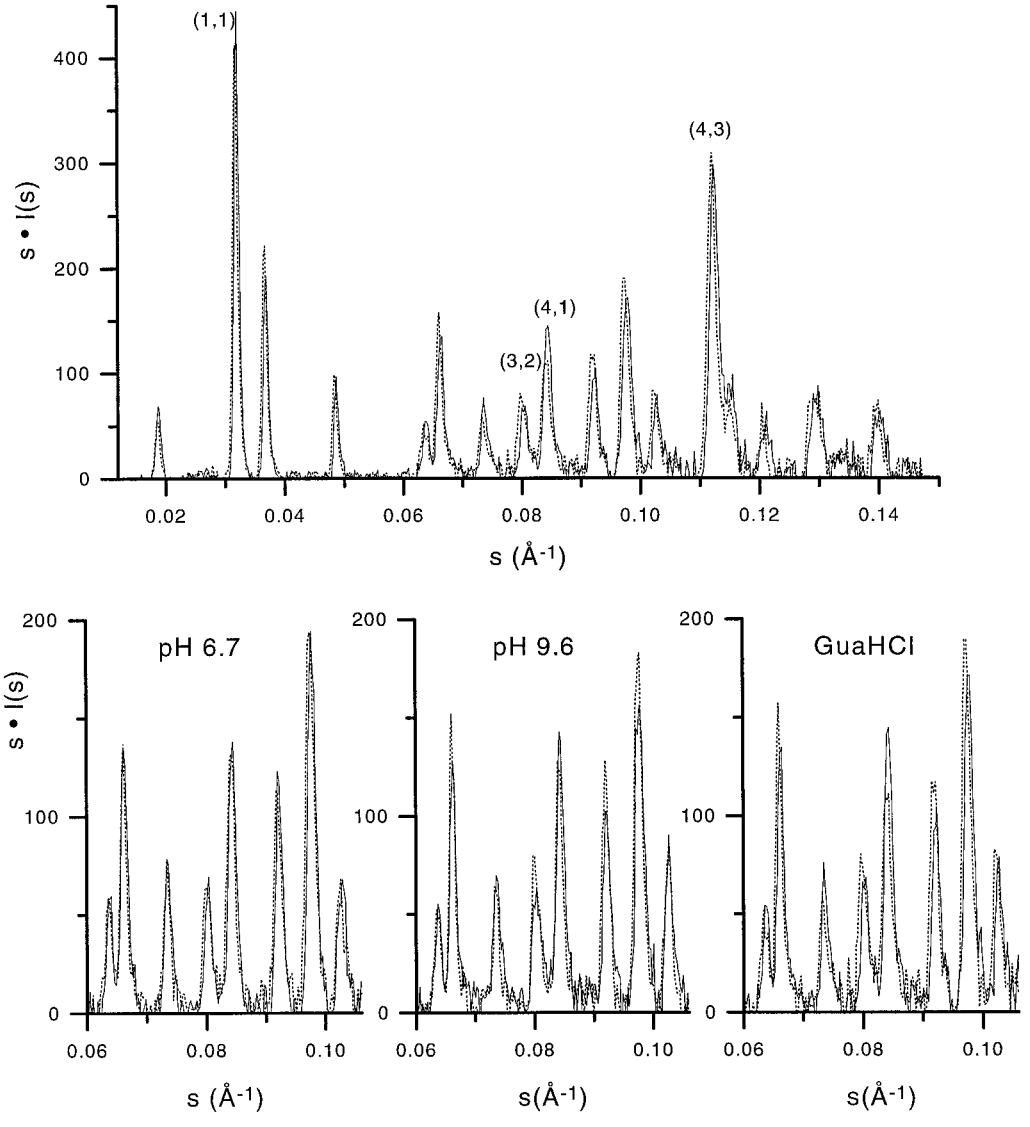

FIGURE 2 Lorentz-corrected x-ray diffraction patterns of BR-ASP38ARG purple membranes at 100% r.h. (*Top*) Light-adapted ground state (——) and illuminated sample (·····) of a PM film incubated with GuaHCl (pH 9.6). (*Bottom*) Range from reflection (2, 2) to (5, 1) under different conditions on an expanded scale. Left: pH 6.7 (around −6°C); center: pH 9.6 (around +6°C); right: pH 9.6 + GuaHCl (around +6°C). The shift of diffraction peaks to lower *s* values corresponding to an increase in the lattice constant for films under illumination is clearly visible for all samples. $s = 2\sin\Theta/\lambda$, with Bragg angle Θ and wavelength $\lambda = 1.5$ Å.

in the M state is more temperature dependent. The characteristic changes in the (3, 2) and (4, 1) reflections are slightly more pronounced in the presence of GuaHCl, as a result of the expected larger number of molecules accumulated in M_2.

The corresponding difference electron density projections are depicted in Fig. 3. They confirm that only at pH 9.6 do the continuously illuminated samples with and without GuaHCl display the previously determined changes mainly at helices F and G. The sample at pH 6.7, on the other hand, shows not only much smaller difference densities, but also no significant variations at positions in the BR molecule known to be involved in the larger structural changes. This is most obvious in the vicinity of helix G, where the most pronounced positive difference density is found in the maps of the other samples. Morever, the difference densities near helix F are increased at higher pH for both samples. The most likely explanation for the observed differences is that the M_2 state accumulates at pH 9.6 with the characteristic changes of helix G and the outward tilt of helix F (Dencher et al., 1989; Koch et al., 1991; Subramaniam et al., 1993), whereas the M_1 state is enriched at pH 6.7. Because small positive difference densities are also detectable in the region of helices B, E, and F in the latter sample, it is possible that the M_1 state also displays small structural changes compared to the ground state, without showing the pronounced changes in the tertiary structure visible at high pH with and without GuaHCl.

This finding is consistent with the separation of the M state into two states, M_1 and M_2, of which only the M_2 state displays the characteristic large structural changes (Varo and Lanyi, 1991, 1995; Sass et al., 1997). The smaller structural changes in the sample at pH 6.7 are in accordance with the previous interpretation that structural changes between the intermediates are not a single-step event. The smaller changes prepare the large changes in the tertiary structure (Sass et al., 1997). In this respect it is noteworthy that the lattice constant of the low-pH sample also increases upon illumination (s. Fig. 2) and is therefore already present in the M_1 state. Thus this lattice constant increase of ~0.2 Å is completed before the large alterations at helices F and G become visible in the difference electron density map (Fig. 3).

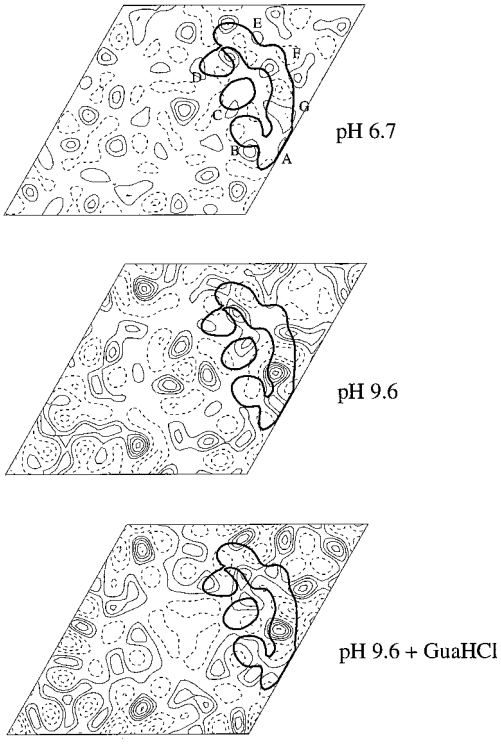

FIGURE 3 Difference electron density maps (M state minus light-adapted ground state) of the BR-ASP38ARG PM at 100% r.h. under different conditions. (*Top*) pH 6.7, M_1 state. (*Center*) pH 9.6, M_2 state. (*Bottom*) pH 9.6, incubated with GuaHCl, M_2 state. The bold contour outlines the BR monomer; individual helices are marked by capital letters from A to G. Continuous lines correspond to positive, dashed lines to negative electron density levels. Contour levels are on the same scale in all maps.

FTIR measurements

To further characterize the differences between M intermediates detected by diffraction experiments, FTIR difference spectra of comparable samples were measured (Figs. 4 and 5). The spectra have a difference band pattern characteristic of the M intermediate, i.e., the deprotonation of the Schiff base (a positive band at 1624 cm^{-1} and a negative band at 1639 cm−1), the protonation of Asp85 (a positive band at or near 1761 cm^{-1}), and the typical fingerprint region (no positive band at 1186 cm^{-1}) (Braiman et al., 1987; Gerwert et al., 1989). Fig. 4 (*top*) shows that upon cooling, the difference band pattern of the FTIR spectrum of the sample at pH 6.7 does not change appreciably. Only the intensities of the difference bands increase at lower temperature, indicating that under identical conditions of continuous illumination, more BR molecules are trapped in the M state. The most pronounced differences between the FTIR spectra of the samples at different pH are in the amide I region 1670–1660 cm^{-1} (Figs. 4 and 5). The ASP38ARG sample at pH 6.7 (Figs. 4 and 5) displays, as already reported by Riesle et al. (1996), a very small difference band at 1670 cm^{-1} and only a small negative one at 1660 cm^{-1}. The ASP38ARG sample at pH 9.6, with and without GuaHCl (Fig. 4), on the other hand, shows a negative difference band at 1670 cm^{-1} and a shoulder, i.e., a smaller band, at 1660 cm^{-1}. This is another indication, albeit somewhat controversial (Ormos, 1991; Ormos et al., 1992; Perkins et al., 1992; Vonck et al., 1994; Sass et al., 1997; Hessling et al., 1997), that the sample at pH 6.7 is accumulated in the M_1 state, whereas the samples at higher pH with and without GuaHCl are trapped in the M_2 state (Fig. 5). The amide II region, 1540–1560 cm^{-1}, also presents the characteristic differences between the two M states: a less pronounced broad difference band for the M_1 state and a stronger band peaked at 1557 cm^{-1} for the M_2 state (Ormos, 1991; Sass et al., 1997).

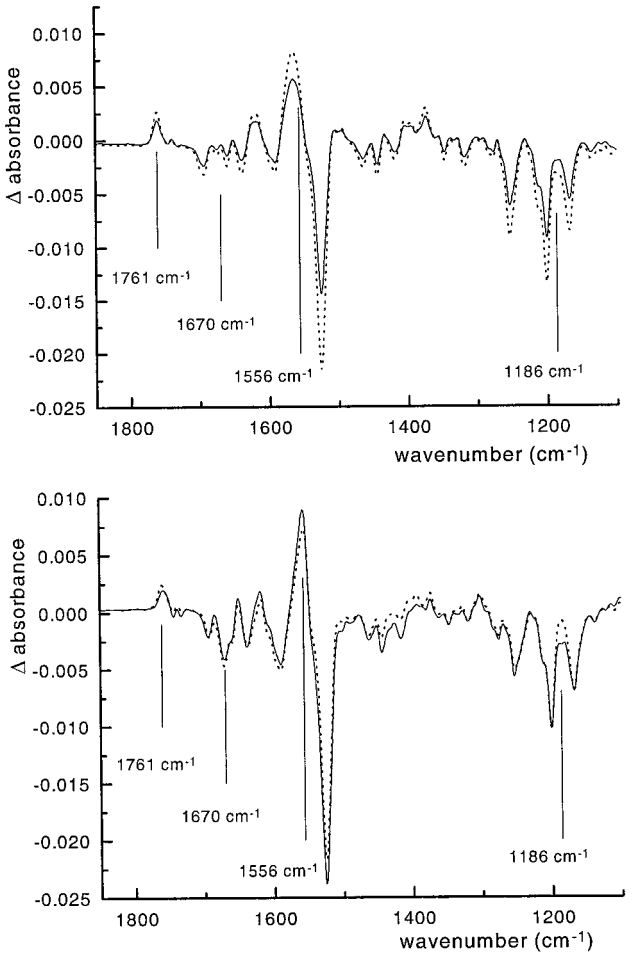

FIGURE 4 FTIR difference spectra (M state minus light-adapted ground state). (*Upper spectra*) BR-ASP38ARG (pH 6.7, 100% r.h.) at 20°C (——) and 10°C (·····). The larger differences at the lower temperature show the higher degree of accumulation of the same M state. (*Lower spectra*) BR-ASP38ARG (pH 9.6, 20°C, 100% r.h., scaled) with (——) and without (·····) the addition of GuaHCl.

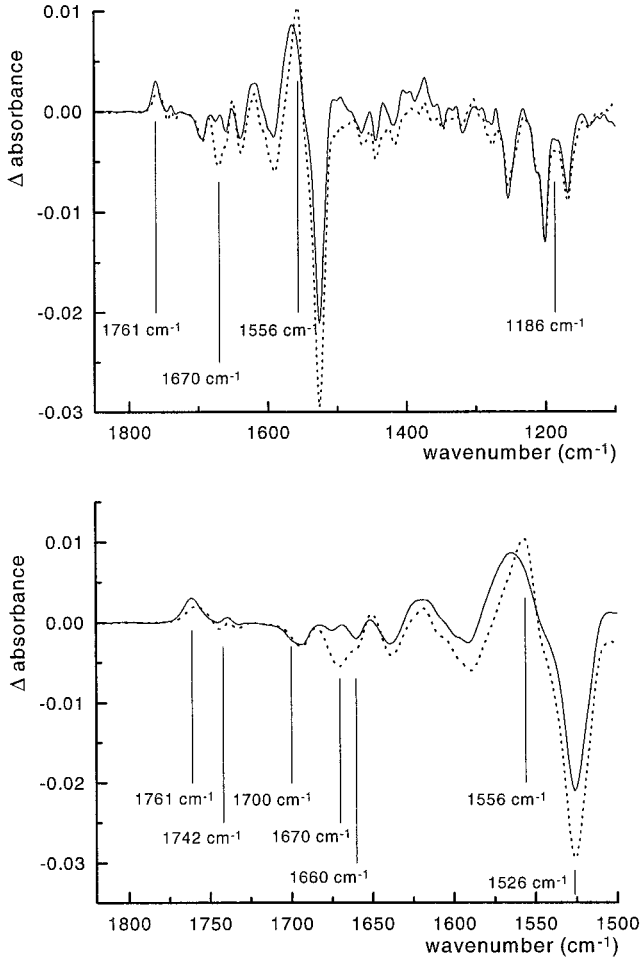

FIGURE 5 FTIR difference spectra (M state minus light-adapted ground state). (*Upper spectra*) BR-ASP38ARG (100% r.h.), pH 6.7 (——) and pH 9.6 with GuaHCl (·····). (*Lower spectra*) An expanded region of the upper spectra.

In addition, the difference band of Asp85 clearly indicates a correlation with the changes in the structure detected by the diffraction experiment. The band at 1761 cm^{-1} for the pH 6.7 sample is broadening/shifting toward 1755 cm^{-1} for the sample at pH 9.6. This indicates that the postulated alteration in the environment leading to the shift of the difference band toward 1755 cm^{-1} (Braiman et al., 1991; Pfefferle et al., 1991; Sasaki et al., 1994) takes place with the transition from the M_1 to the M_2 state.

In agreement with our investigations on wt BR (Sass et al., 1997), the results in Fig. 5 confirm that the sample incubated with GuaHCl under continuous illumination is trapped in a state with a deprotonated Asp96, as indicated by the negative difference band at 1742 cm^{-1} (Gerwert et al., 1989; Braiman et al., 1991; Sasaki et al., 1994). In the region of 1700 cm^{-1}, assigned to be indicative for the deprotonation of Glu204 (Brown et al., 1995), no difference is detectable between the samples at pH 6.7 and pH 9.6. This indicates that, if this residue is the proton-releasing group, it is already deprotonated in the M_1 state, i.e., the proton is released from the extracellular protein surface during the transition from the L to the M_1 state.

CONCLUSIONS

The results obtained with the ASP38ARG-BR mutant support the idea that large tertiary structural changes are not associated with the transition from the L to the M intermediate, but with the transition from the M_1 to the M_2 state. The detectable large changes in the structure take place after the deprotonation of the Schiff base, as could be demonstrated in a diffraction experiment for the ASP85ASN-BR mutant (Brown et al., 1997), and after the release of the proton at the extracellular side. This implies that the structural changes follow a redistribution of charges. This model is also supported by the recent observation of the influence of an externally applied electrical field on the ratio of the M_1 to M_2 state (Nagel et al., 1998). Because the charge displacements responsible for the transition from the M_1 to

the M_2 state involve at least the region of the Schiff base and the extracellular side of BR, changes in the global charge pattern could also explain the long-lived M_1 state of this mutant at pH 6.7. The substitution of an arginine for an aspartic acid makes the charge pattern at the cytoplasmic side more positive, either directly by the positive charge of the arginine or indirectly but more effectively, because another positive charge is no longer compensated for by the interaction with the aspartic acid. This new charge pattern, more positive at the cytoplasmic side than in wt BR, could interfere with the charge variation resulting from the deprotonation of the Schiff base and therefore slow down the large structural rearrangements. This would result in the accumulation of the M_1 state. Because no large structural changes are detectable under this condition, and if one assumes a sequential order of M_1 and M_2, the general conclusion for wt BR can be drawn that a charge redistribution around the Schiff base and at the extracellular side of the molecule results in an altered force field within BR, which drives the large structural changes.

At a pH above 9, another group on the cytoplasmic side might be deprotonated and at least partly compensate for the added positive charge of the arginine. This would allow the structural changes associated with the transition to the M_2 state to take place. The transition to the subsequent photocycle intermediates N and O, however, would then also be slowed down as a result of this global charge distribution and/or because of the lack of protons necessary for the reprotonation of the Schiff base. Additional changes in the structure that are not detectable in ASP38ARG-BR under the used conditions seem to be necessary for the transition to the N intermediate. This is indicated by the less pronounced changes in the FTIR difference bands at 1670 and 1650 cm^{-1} for the M state trapped in the mutant in the presence of GuaHCl, as compared to the M_G state accumulated under identical conditions with wt BR (Sass et al., 1997).

Another important conclusion is that also for ASP38ARG-BR, for which no indications for structural changes were found in time-resolved FTIR experiments at pH 6.7 (Riesle et al., 1996), the known structural variations during the photocycle take place. The intermediates that display these changes accumulate only under specific experimental conditions. At pH 6.7, the relaxation of the structural alteration after the extended period in the M_1 state is too fast to be detectable. At pH 9.6, on the other hand, it is not the structural change that limits, but the steps following it. The photocycle of ASP38ARG is therefore retarded in a state similar to that previously found in the mutant ASP96ASN-BR (Koch et al., 1991; Subramaniam et al., 1993), i.e., the M_2 state with the characteristic alterations in the tertiary structure. Therefore, if one assumes that the same sequence of events takes place in the photocycle of this mutant at pH values above and below 9, vectorial proton pumping in this mutant also seems to be dependent on tertiary structural changes which, however, can only be observed under the appropriate kinetic conditions.

We thank Dr. J. Heberle for helpful comments and provision of the FTIR spectrometer.

This work was supported by the Deutsche Forschungsgemeinschaft (SFB 472/P3 to NAD and SFB 189/B12, B15 to GB); the Bundesministerium für Bildung, Wissenschaft, Forschung und Technologie (03-DE4DAR-1 to NAD and GB); and the Fonds der Chemischen Industrie (to NAD).

REFERENCES

Boulin, C. J., R. Kempf, A. Gabriel, and M. H. J. Koch. 1988. Data acquisition systems for linear and area x-ray detectors using delay line readout. *Nucl. Instrum. Methods.* A269:312–320.

Braiman, M. S., P. L. Ahl, and K. J. Rothschild. 1987. Millisecond Fourier-transform infrared difference spectra of bacteriorhodopsin's M_{412} photoproduct. *Proc. Natl. Acad. Sci. USA.* 84:5221–5225.

Braiman, M. S., O. Bousche, and K. J. Rothschild. 1991. Protein dynamics in the bacteriorhodopsin photocycle: submillisecond Fourier transform infrared spectra of the L, M and N photointermediates. *Proc. Natl. Acad. Sci. USA.* 88:2388–2392.

Brown, L. S., H. Kamikubo, L. Zimanyi, M. Kataoka, F. Tokunaga, P. Verdegem, J. Lugtenburg, and J. K. Lanyi. 1997. A local electronic change is the cause of the large-scale protein conformation shift in bacteriorhodopsin. *Proc. Natl. Acad. Sci. USA.* 94:5040–5044.

Brown, L. S., J. Sasaki, H. Kandori, A. Maeda, R. Needleman, and J. K. Lanyi. 1995. Glutamic acid 204 is the terminal proton release group at the extracellular surface of bacteriorhodopsin. *J. Biol. Chem.* 270: 27122–27126.

Dencher, N. A., D. Dresselhaus, G. Zaccai, and G. Büldt. 1989. Structural changes in bacteriorhodopsin during proton translocation revealed by neutron diffraction. *Proc. Natl. Acad. Sci. USA.* 86:7876–7879.

Ebrey, T. G. 1993. Light energy transduction in bacteriorhodopsin. *In* Thermodynamics of Membrane Receptors and Channels. M. B. Jackson, editor. CRC Press, Boca Raton, FL. 353–387.

Fodor, S. P., J. B. Ames, R. Gebhard, E. M. van den Berg, W. Stoeckenius, J. Lugtenburg, and R. Mathies. 1988. Chromophore structure in bacteriorhodopsin's N intermediate: implications for the proton-pumping mechanism. *Biochemistry.* 27:7079–7101.

Gabriel, A., and F. Dauvergne. 1982. The localisation method used at EMBL. *Nucl. Instrum. Methods.* 201:203–204.

Gerwert, K., B. Hess, J. Soppa, and D. Oesterhelt. 1989. Role of aspartate-96 in proton translocation by bacteriorhodopsin. *Proc. Natl. Acad. Sci. USA.* 86:4943–4947.

Grigorieff, N., T. A. Ceska, K. H. Downing, J. M. Baldwin, and R. Henderson. 1996. Electron-crystallographic refinement of the structure of bacteriorhodopsin. *J. Mol. Biol.* 259:393–421.

Haupts, U., J. Tittor, E. Bamberg, and D. Oesterhelt. 1997. General concept for ion translocation by halobacterial retinal proteins: the isomerization/switch/transer (IST) model. *Biochemistry.* 36:2–7.

Hauss, T., G. Büldt, M. P. Heyn, and N. A. Dencher. 1994. Light-induced isomerisation causes an increase in the chromophore tilt in the M-intermediate of bacteriorhodopsin: a neutron diffraction study. *Proc. Natl. Acad. Sci. USA.* 91:11854–11858.

Henderson, R., J. M. Baldwin, K. H. Downing, J. Lepault, and F. Zemlin. 1986. Structure of purple membrane from *Halobacterium halobium*: recording, measurement and evaluation of electron micrographs at 3.5 Å resolution. *Ultramicroscopy.* 19:147–178.

Hessling, B., J. Herbst, R. Rammelsberg, and K. Gerwert. 1997. Fourier transform infrared double-flash experiments resolve bacteriorhodopsin's M_1 to M_2 transition. *Biophys. J.* 73:2071–2080.

Kamikubo, H., M. Kataoka, G. Varo, T. Oka, F. Tokunaga, R. Needleman, and J. K. Lanyi. 1996. Structure of the N intermediate of bacteriorhodopsin revealed by x-ray diffraction. *Proc. Natl. Acad. Sci. USA.* 93: 1386–1390.

Kimura, Y., D. G. Vassylyev, A. Miyazawa, A. Kidera, M. Matsushima, K. Mitsuoka, K. Murata, T. Hirai, and Y. Fujiyoshi. 1997. Surface of bacteriorhodopsin revealed by high-resolution electron crystallography. *Nature.* 389:206–211.

Koch, M. H. J., N. A. Dencher, D. Oesterhelt, H.-J. Ploehn, G. Rapp, and G. Büldt. 1991. Time-resolved x-ray diffraction study of structural changes associated with the photocycle of bacteriorhodopsin. *EMBO J.* 10:521–526.

Lanyi, J. K. 1995. Bacteriorhodopsin as a model for proton pumps. *Nature.* 375:461–463.

Nagel, G., B. Kelety, B. Möckel, G. Büldt, and E. Bamberg. 1998. Voltage dependence of proton pumping by bacteriorhodopsin is regulated by the voltage sensitive ratio of M_1 to M_2. *Biophys. J.* 74:403–412.

Nagle, J. F., L. A. Parodi, and R. H. Lozier. 1982. Procedure for testing kinetic models of the photocycle of bacteriorhodopsin. *Biophys. J.* 38:161–174.

Nakasako, M., M. Kataoka, Y. Amemiya, and F. Tokunaga. 1991. Crystallographic characterization by x-ray diffraction of the M-intermediate from the photocycle of bacteriorhodopsin at room temperature. *FEBS Lett.* 292:73–75.

Oesterhelt, D., J. Tittor, and E. Bamberg. 1992. A unifying concept for ion translocation by retinal proteins. *J. Bioenerg. Biomembr.* 24:181–191.

Ormos, P. 1991. Infrared spectroscopic demonstration of a conformational change in bacteriorhodopsin involved in proton pumping. *Proc. Natl. Acad. Sci. USA.* 88:473–477.

Ormos, P., K. Chu, and J. Mourant. 1992. Infrared study of the L, M, and N intermediates of bacteriorhodopsin using the photoreaction of M. *J. Biochem.* 31:6933–6937.

Pebay-Peyroula, E., G. Rummel, J. P. Rosenbusch, and E. M. Landau. 1997. X-ray structure of bacteriorhodopsin at 2.5 Å from microcrystals grown in lipidic cubic phases. *Science.* 277:1676–1681.

Perkins, G. A., E. Liu, F. Burkard, E. A. Berry, and R. M. Glaeser. 1992. Characterization of the conformational change in the M_1 and M_2 substates of bacteriorhodopsin by the combined use of visible and infrared spectroscopy. *J. Struct. Biol.* 109:142–151.

Pfefferle, J., A. Maeda, J. Sasaki, and A. Maeda. 1991. Fourier transform infrared study of the N intermediate of bacteriorhodopsin. *Biochemistry.* 30:6548–6556.

Riesle, J., D. Oesterhelt, N. A. Dencher, and J. Heberle. 1996. D38 is an essential part of the proton translocation pathway in bacteriorhodopsin. *Biochemistry.* 35:6635–6643.

Sasaki, J., J. K. Lanyi, R. Needleman, T. Yoshizawa, and A. Meada. 1994. Complete identification of C═O stretching vibrational bands of protonated aspartic acid residues in the difference infrared spectra of M and N intermediates versus bacteriorhodopsin. *Biochemistry.* 33:3178–3184.

Sasaki, J., Y. Shichida, J. K. Lanyi, and A. Maeda. 1992. Protein changes associated with reprotonation of the Schiff base in the photocycle of Asp^{96}. *Biol. Chem.* 267:20782–20786.

Sass, H. J., I. W. Schachowa, G. Rapp, M. H. J. Koch, D. Oesterhelt, N. A. Dencher, and G. Büldt. 1997. The tertiary structural changes in bacteriorhodopsin occur between M states: x-ray diffraction and Fourier transform infrared spectroscopy. *EMBO J.* 16:1484–1491.

Schulten, K., and P. Tavan. 1978. A mechanism for the light-driven proton pump of *Halobacterium halobium*. *Nature.* 272:85–86.

Souvignier, G., and K. Gerwert. 1992. Proton uptake mechanism of bacteriorhodopsin as determined by time-resolved stroboscopic-FTIR-spectroscopy. *Biophys. J.* 63:1393–1405.

Subramaniam, S., M. Gerstein, D. Oesterhelt, and R. Henderson. 1993. Electron diffraction analysis of structural changes in the photocycle of bacteriorhodopsin. *EMBO J.* 12:1–8.

Varo, G., and J. K. Lanyi. 1991. Kinetic and spectroscopic evidence for an irreversible step between deprotonation and reprotonation of the Schiff base in the bacteriorhodopsin photocycle. *Biochemistry.* 30:5008–5015.

Varo, G., and J. K. Lanyi. 1995. Effects of hydrostatic pressure on the kinetics reveal a volume increase during the bacteriorhodopsin photocycle. *Biochemistry.* 34:12161–12169.

Vonck, J. 1996. A three-dimensional difference map of the N intermediate in the bacteriorhodopsin photocycle: part of the F helix tilts in the M to N transition. *Biochemistry.* 35:5870–5878.

Vonck, J., B.-G. Han, F. Burkard, G. A. Perkins, and R. M. Glaeser. 1994. Two progressive substates of the M-intermediated can be identified in glucose-embedded, wild-type bacteriorhodopsin. *Biophys. J.* 67:1173–1178.